Available online at www.sciencedirect.com
SCIENCE DIRECT®
Ultrasonics 42 (2004) 647–651
Ultrasonics
www.elsevier.com/locate/ultras

Surface acoustic wavefront sensor using custom optics

Steve D. Sharples *, Matthew Clark, Mike Somekh

Applied Optics, Electrical and Electronic Engineering, University of Nottingham, University Park, Nottingham NG7 2RD, UK

Abstract

We have designed and had manufactured a custom surface acoustic wavefront sensor, using a standard CMOS process. Ultrasound propagating along the surface of an object perturbs the reflection of incident laser light, which has been focused onto the object using a cylindrical lens. These high-frequency angular perturbations of reflected light relate to the amplitude and phase of the ultrasound along a line on the surface of the object, and thus correspond to the acoustic wavefront. The reflected light is imaged onto a custom linear array of split photodiodes; these simultaneously detect the high-frequency perturbations at several discrete points along the line, forming an acoustic wavefront sensor.

As well as a description of the device, its role within an adaptive optical scanning acoustic microscope is discussed. The sensor detects the distortions to the acoustic wavefront after it has propagated through an aberrating medium, such as a metal containing grains of random orientation. The information attained may then be used to alter the generation profile of the optical generation source of the acoustic waves, thus reducing the distortion caused by the aberration and increasing the resolution and accuracy of the system as a whole.
© 2004 Elsevier B.V. All rights reserved.

Keywords: Acoustic sensors; Acoustic aberrations; Aberration correction; SAW; Laser ultrasound

1. Introduction

A wavefront propagating through an aberrating medium is affected in some way by the medium. The concept of adaptive optical correction for imaging distant stars through the Earth's turbulent atmosphere is well known [1]. The correction involves detecting the aberrated wavefront, using either a nearby guide star or a guide laser reflected off the upper atmosphere as a reference. The difference between the aberrated wavefront and the ideal case is used to correct the focus by altering the shape of the telescope mirror. Ultrasound waves propagating through an anisotropic media are also aberrated. If the material consists of grains of random orientation—such as metals—the acoustic wavefront is aberrated because of velocity variations in the material microstructure.

In this paper we present details of an acoustic wavefront sensor (AWFS) that is able to detect the surface acoustic wave (SAW) wavefront as it propagates, with the aim of using the information collected by the sensor to allow for the correction of the aberration, by adjusting the SAW excitation profile.

The AWFS has been integrated into an all-optical scanning acoustic microscope (O-SAM), which has been described previously [2–4]. The O-SAM is capable of rapid, high resolution, nondestructive vector contrast imaging of SAWs without any measurement perturbation or contamination of the sample surface. Fundamentally, light from a reasonably high-powered Q-switched mode locked laser—fundamental frequency 82 MHz, with harmonics extending beyond 1 GHz—is imaged onto the surface of a material, typically in the form of a concentric set of arcs, spaced to match the wavelength of the acoustic waves on the material. In the case of isotropic materials, these acoustic waves propagate to a diffraction-limited focus, where their amplitude and phase is measured by another laser, using a simple modified knife edge detection technique. It is this knife edge detector that is to be replaced by the acoustic wavefront sensor.

* Corresponding author. Fax: +44-0115-9515616.
E-mail address: steve.sharples@nottingham.ac.uk (S.D. Sharples).

0041-624X/$ - see front matter © 2004 Elsevier B.V. All rights reserved.
doi:10.1016/j.ultras.2004.01.044

2. Effects of material aberrations

Fig. 1 illustrates schematically and experimentally the effect that material anisotropy has on the propagation of focused acoustic waves.

The upper images in the figure illustrate the propagation of focused SAWs on an isotropic medium—the upper right hand image shows an aerial point spread function (PSF) taken on aluminium-coated glass at 82 MHz. This image was acquired with the O-SAM instrument by fixing the relative positions of the sample and the excitation profile, and raster-scanning the detection point. The location of the intended SAW detection point is also marked in the figure, although its size has been exaggerated for clarity. The lower images of Fig. 1 illustrate the propagation of focused SAWs on a multi-grained anisotropic medium—the lower right hand image is an aerial PSF taken on aluminium. Not only does the majority of the acoustic energy miss the geometric focus of the excitation arcs, but the PSF has clearly broadened and dispersed.

In its normal mode of operation, the O-SAM acquires SAW c-scan images by detecting the surface waves at the acoustic focus—fixing the relative positions of the excitation source and the detection point—and raster-scanning the material. Material anisotropy affects the quality of the images obtained [2,5] because the acoustic energy is no longer focused to the detection point. This has important implications in nondestructive testing applications, where the acoustic energy is not probing the intended parts of the material. The 'signal drop-out' does not occur due to attenuation or scattering, rather because the acoustic energy has been displaced.

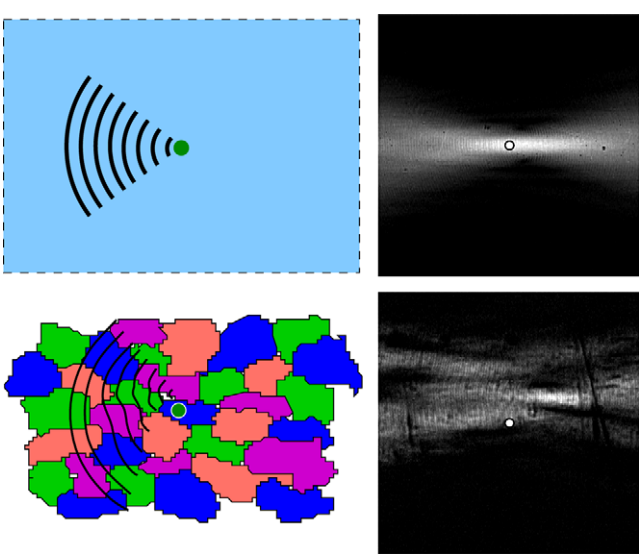

Fig. 1. The upper images illustrate the propagation of SAWs on an isotropic medium—the upper right hand image is an aerial PSF taken on aluminium-coated glass. The lower images illustrate the propagation of focused SAWs on a multi-grained anisotropic medium—the lower right hand image is an aerial PSF taken on aluminium.

3. Correcting for the effects of aberrations

To correct for the effects of material aberrations we require knowledge of the effects of the aberrations, and a method of adjusting the excitation profile to correct for them. The principle is illustrated in Fig. 2.

In the case of the O-SAM instrument, we use a spatial light modulator (SLM) to achieve the excitation profile adjustment [2,3]. We have previously shown that if it is possible to acquire the complex amplitude of the PSF on the plane perpendicular to the propagation direction at the desired point of detection, then it is possible to use this information to generate a new excitation profile to redirect the acoustic waves back to the detection point. In the case of weakly aberrating materials, this may be achieved by simply 'tilting' the arc excitation profile, to steer the acoustic energy back to its intended destination [2]. A higher-order correction technique [6] is required to correct for aberrations that break up the wavefront as well as displacing it. This technique involves the back-propagation of the measured acoustic field using an angular spectrum propagation technique [7], where the phase error is calculated compared to the geometric excitation profile. This error is then used to generate a new excitation profile.

In both cases shown previously, the wavefront information was acquired by scanning a single point detector across acoustic focus using a mechanical stage. This needs to be done for each point in a c-scan image (although there is obviously a certain degree of correlation between nearby points) and adds a significant overhead to the data acquisition time. It was shown in [6] that 16 discrete points along the PSF was sufficient—even with poor signal to noise ratios—to achieve successful higher-order correction.

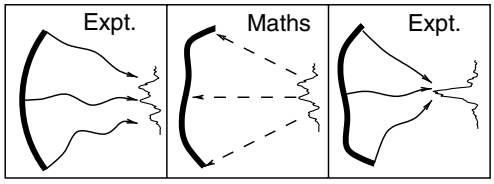

Fig. 2. The figure illustrates schematically the process of higher order wavefront correction. The aberrated wavefront is acquired in the left hand part of the figure. This is back propagated to the excitation region (centre) and the difference between this and the geometrical ideal is then used as the excitation pattern (right hand side).

4. The acoustic wavefront sensor (AWFS)

At the heart of the acoustic wavefront sensor developed is a 16×2 array of photodetectors, designed and constructed using a standard 0.7 μm CMOS process. An optical image of the photodiode array is shown in Fig. 3.

The optical image was acquired by scanning a focused laser beam over the device and measuring the amount of light reflected. This method allowed us to accurately measure the response of each photodiode. The pitch of the array is 100 μm per pixel, and the array was designed such that the gap between each half of a pair of photodiodes is as small as possible, and is 4 μm. The area immediately surrounding the photodiode array is covered with a metal layer, to prevent stray light from areas outside the array producing photocurrent in nearby pixels.

The efficiency of the photodiodes is approximately 0.35 A/W for incident light at 532 nm (the wavelength used in the O-SAM instrument for detection). Although the full bandwidth of the device has not yet been ascertained, it is capable of detecting acoustic waves at a frequency of 328 MHz, as shown in Fig. 4. This signal was acquired by focusing the light onto just one pair of photodiodes on the array. Some electronic filtering was used to eliminate some of the noise, but the signal is otherwise real time.

Each pair of photodiodes in the 16×2 array measures the angular displacement of a focused beam reflected from the sample surface, as it is perturbed by the surface acoustic waves—the AWFS is therefore a 16 channel knife edge detector. Its place within the O-SAM instrument is illustrated schematically in Fig. 5.

A green laser is focused onto the sample at the acoustic focus using a standard lens. A slight astigmatism is added by the addition of a weak cylindrical lens, to produce a line approximately 400 μm long on the

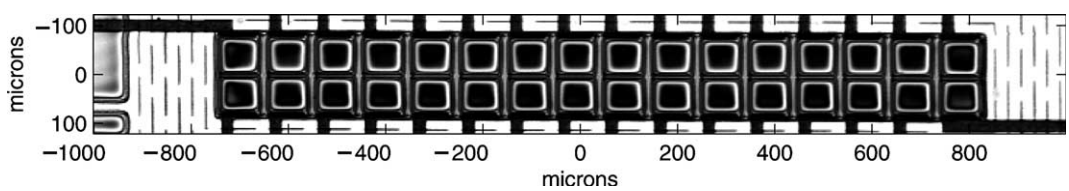

Fig. 3. Optical image of the array of photodetectors on the AWFS device. The device is designed and manufactured using a standard CMOS process. The optical image was acquired by scanning a focused laser beam over the device and measuring the amount of light reflected.

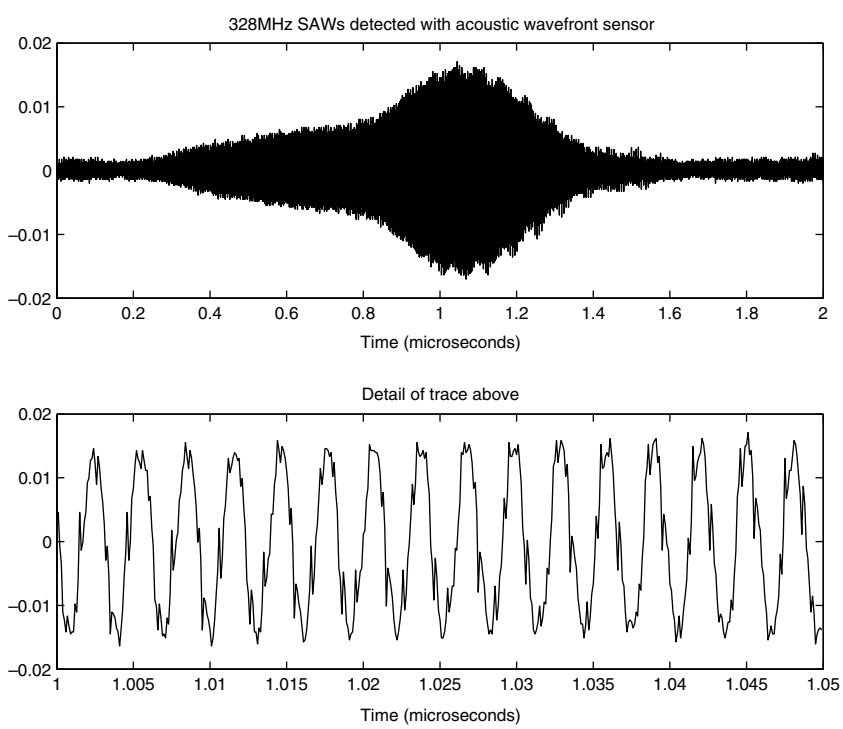

Fig. 4. A real-time 328 MHz acoustic signal detected by one channel of the acoustic wavefront sensor. The signal has been filtered electronically. A detail of the signal is also shown.

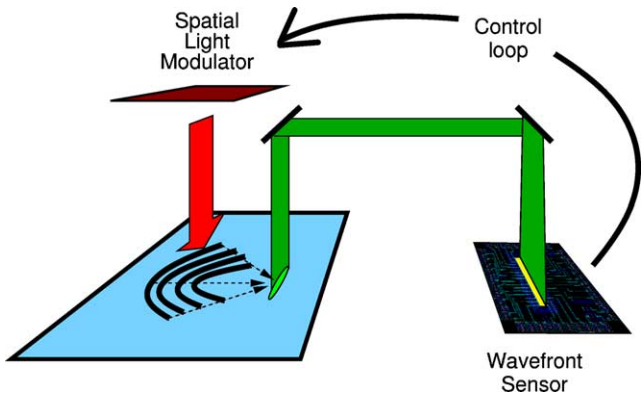

Fig. 5. Schematic of the all-optical scanning acoustic microscope, employing a spatial light modulator to control the SAW excitation profile, and an acoustic wavefront sensor to acquire information about the SAWs as they propagate.

sample surface that is diffraction limited in the orthogonal direction—the direction of SAW propagation. This line is then imaged onto the AWFS using another set of lenses. As different parts of the line on the sample are perturbed by the acoustic wavefront, the perturbations are detected by elements of the 16 channel array according to their position.

5. Results

The integration of the AWFS into the O-SAM is still at a very early stage at the time of writing. Rather than image the line across the entire 16 element array, the line is imaged onto just five adjacent elements. Nevertheless, Fig. 6 illustrates some of the potential of the sensor as part of the instrument as a whole.

The figure shows a schematic representation of the locations of the SAW excitation profile, the five points at which the AWFS measures the acoustic wavefront, and the approximate location and size of the acoustic focus. The outputs of the five wavefront sensor elements are shown in the right of the figure. The upper and lower parts of the figure illustrate the sensor outputs for two different excitation profiles.

The spacing of the excitation pattern was chosen to produce 82 MHz SAWs on the sample used, a piece of aluminium-coated glass. The signals shown in the figure are the result of 50 coherent averages. This is necessary because the signal to noise ratio is significantly poorer on the outer elements—this in turn is due to the Gaussian distribution of optical energy along the detection line. This effect could be eliminated by using a computer generated hologram [8] to produce a line of uniform intensity across the desired region, or reduced by making

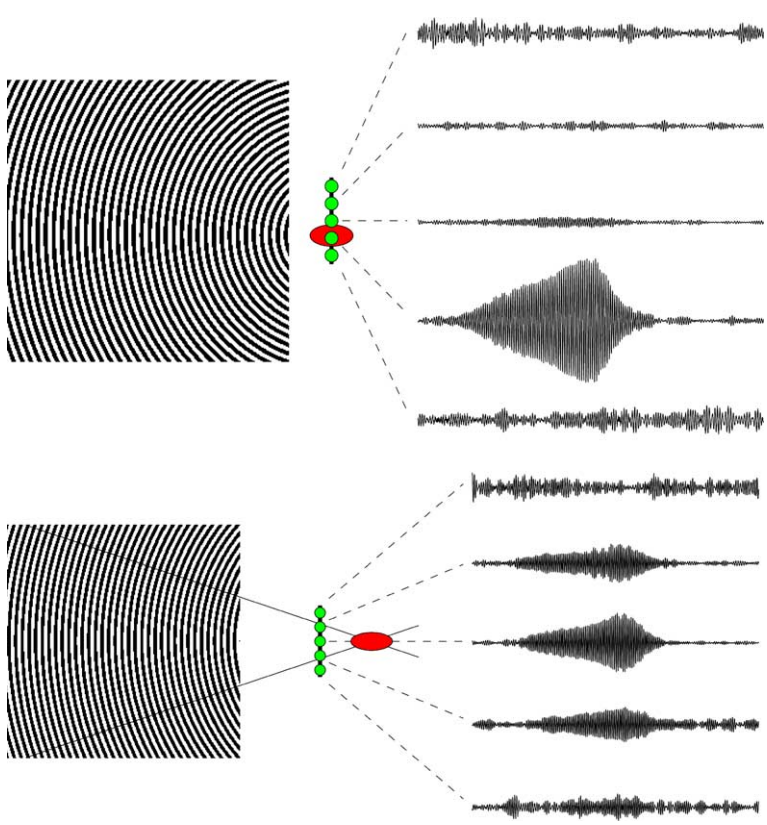

Fig. 6. Simultaneous detection of SAW wavefront at five points using AWFS, for two different SAW excitation profiles. The relative positions of the excitation profile, the five detection regions, and the approximate location of the acoustic focus are shown schematically in the figure.

the line longer than required, and only imaging the central—relatively uniform—section onto the AWFS.

6. Conclusions

The results presented are, as stated, early results from a system in the first stages of development. Nevertheless they illustrate that simultaneous detection of a SAW wavefront at several discrete points is possible with an acoustic wavefront sensor that has been designed and constructed using a standard CMOS process. The use of this standard process, routinely used for analogue and digital circuits, is the key to the sensor's future potential. It allows the associated detection electronics to be constructed on the same piece of silicon as the photodiodes, to form an integrated optical sensor [9]. This significantly reduces much of the complexity, cost and variability of a multi-channel detector system.

Acknowledgements

We would like to acknowledge the support of the RCDNE, EPSRC and Rolls Royce Aeroengines for their continued support.

References

[1] R.K. Tyson, Principles of Adaptive Optics, Academic Press, 1991.
[2] S.D. Sharples, M. Clark, M.G. Somekh, All-optical adaptive scanning acoustic microscope, Ultrasonics 41 (4) (2003) 295–299.
[3] S.D. Sharples, M. Clark, M. Somekh, Efficient and flexible laser ultrasound generation using spatial light modulators, Electronics Letters 37 (18) (2001) 1145–1146.
[4] M. Clark, S.D. Sharples, M. Somekh, Laser ultrasonic microscopy, Materials Evaluation 60 (9) (2002) 1094–1098.
[5] M. Clark, S.D. Sharples, M.G. Somekh, Fast all-optical Rayleigh wave microscope: Imaging on isotropic and anisotropic materials, IEEE Transactions on Ultrasonics, Ferroelectrics and Frequency Control 47 (1) (2000) 65–74.
[6] S.D. Sharples, M. Clark, M.G. Somekh, Dynamic higher-order correction of acoustic aberration due to material microstructure, Applied Physics Letters 81 (12) (2002) 2288–2290.
[7] J.W. Goodman, Introduction to Fourier Optics, McGraw-Hill, 1968.
[8] M. Clark, R. Smith, A direct-search method for the computer design of holograms, Optics Communications 124 (1–2) (1996) 150–164.
[9] B.H. Pui, B. Hayes-Gill, M. Clark, M. Somekh, C. See, J.F. Pieri, S.P. Morgan, A. Ng, The design and characterisation of an optical VLSI processor for real time centroid detection, Analog Integrated Circuits and Signal Processing 32 (1) (2002) 67–75.